NU Science Journal 2011; 7(2) : 10 – 19

Fabrication and Characterization of $0.904Bi_{0.5}Na_{0.5}TiO_3$-$0.040Bi_{0.5}K_{0.5}TiO_3$-$0.056BaTiO_3$ Lead-Free Ceramics Using the Combustion Technique

Atthakorn Thongtha and Theerachai Bongkarn*
Department of Physics, Faculty of Science, Naresuan University,
Phitsanulok, 65000, Thailand
*Corresponding author. E-mail: researchcmu@yahoo.com

ABSTRACT

A ternary system lead-free piezoelectric ceramic bismuth sodium titanate-bismuth potassium titanate-barium titanate was studied. $(Bi_{0.472}Na_{0.452}K_{0.02}Ba_{0.056})TiO_3$ or $0.904Bi_{0.5}Na_{0.5}TiO_3$-$0.04Bi_{0.5}K_{0.5}TiO_3$-$0.056BaTiO_3$;BNT BKT Bceramics were successfully fabricated using the combustion technique. The effect of sintering temperatures (1050 - 1200 ^oC) on the phase formation, microstructure and dielectric properties of perovskite BNT BKT BT ceramics were studied. XRD results showed the rhombohedral-tetragonal morphotropic phase boundary (MPB). The SEM results showed that the average grain size (1.03-3.49 μm) of samples increased with the increase of sintering temperatures. The samples sintered at the optimum temperature of 1175 ^oC showed the maximum density, shrinkage, dielectric constant at Curie temperature, remanent polarization (P_r), coercive field (E_c) and high piezoelectric constant (d_{33}) were around 5.78 g/cm^3, 17.48%, 5890, 9.5 μC/cm^2, 15.1 kV/cm and 156 pC/N, respectively. The dielectric constant was related to the density of the sintered ceramic.

Keywords: microstructure, lead free piezoelectric ceramics, morphotropic phase boundary, BNT-BKT-BT, combustion technique

Introduction

Recently, lead-free materials with high dielectric and piezoelectric properties have attracted considerable attention to replace the lead containing ferroelectrics. $Bi_{0.5}Na_{0.5}TiO_3$ (BNT) is considered one of the promising lead-free piezoelectric materials due to a large remnant polarization (P_r = 38 μC/cm^2) at room temperature and a high Curie temperature (T_c = 320 ^oC). However, BNT ceramics are difficult to be poled because of their high coercive field (E_c = 73 kV/cm) and high conductivity which causes difficulties in obtaining the desired piezoelectric properties. To solve this problem, $Bi_{0.5}Na_{0.5}TiO_3$-based multi-component solid solution systems have been developed (Takenaka *et al.*, 1991, 1997; Takenaka, 1999; Ichinose and Udagawa, 1995). It has been found that ceramics with good piezoelectric properties can be obtained by the partial substitution of A-site ions $(Bi_{0.5}Na_{0.5})^{2+}$ by Ba^{2+}, $(Bi_{0.5}K_{0.5})^{2+}$ (Chu *et al*., 2002; Elkechai *et al.*, 1996). Among BNT-based solid solutions, the $0.904Bi_{0.5}Na_{0.5}TiO_3$-$0.04Bi_{0.5}K_{0.5}TiO_3$ $0.056BaTiO_3$ system has attracted considerable attention

(Nagata *et al*., 2003) because of a high piezoelectric constant ($d_{33} \approx 140$ pC/N) and a high Curie temperature ($T_c \approx 300\ ^oC$).

Presently, the combustion technique is interesting because it can decrease the calcination and sintered temperature (Thongtha and Bongkarn, 2009), obtain a high density and good electrical properties (Thongtha and Bongkarn, 2010; Julphunthong and Bongkarn, in press). Furthermore, it is well known that optimal sintering conditions lead to ceramics with high dielectric, polarization and piezoelectric properties. However, a detailed study of the synthesis and characterization of $0.904Bi_{0.5}Na_{0.5}TiO_3$-$0.04Bi_{0.5}K_{0.5}TiO_3$-$0.056BaTiO_3$; BNT-BKT-BT ceramics via the combustion technique has not been reported in the literature. So, in this work, the BNT-BKT-BT ceramics were fabricated via the combustion technique. The effect of sintering temperatures on the phase formation, microstructure, dielectric, ferroelectric and piezoelectric properties of BNT-BKT-BT ceramics were also investigated.

Experimental

Bismuth sodium potassium barium titanate [$(Bi_{0.472}Na_{0.452}K_{0.02}Ba_{0.056})TiO_3$ or $0.904Bi_{0.5}Na_{0.5}TiO_3$-$0.04Bi_{0.5}K_{0.5}TiO_3$-$0.056BaTiO_3$; BNT-BKT-BT] powders were synthesized by the combustion technique. For preparation $(Bi_{0.5}Na_{0.5})TiO_3$; BNT powder, the raw materials of Bi_2O_3 (99%), Na_2CO_3 (99%) and TiO_2 (99%) were weighed. A thoroughly ground mixture of raw materials were ground by a ball milling procedure (zirconia milling media under ethanol for 24 h). Drying was carried out at 120 ^{o}C for 4 h. The raw powders were well-mixed with fuel (glycine) in an agate mortar before the calcination step. Afterwards, the uncalcined powders of BNT were calcined at 700 ^{o}C with a dwell time of 1 h and a heating/cooling rate of 5 ^{o}C/min. For synthesis $(Bi_{0.5}K_{0.5})TiO_3$; BKT and $BaTiO_3$; BT, the raw materials of Bi_2O_3 (99%), K_2CO_3, (99%), $BaCO_3$ (99%) and TiO_2 (99%) were weighed in the required stoichiometric ratio and the raw materials were mixed by a ball milling procedure. The processing of BKT and BT powders is similar to BNT powders, but the uncalcined powders of BKT and BT were well-mixed with the fuel (glycine for BKT and urea for BT) and calcined at 850 ^{o}C for 2 h and 1200 ^{o}C for 4 h, respectively.

The calcined powders of BNT, BKT and BT were weighed and mixed in the required stoichiometric ratio with a 2 wt.% binder solution and reground by ball milling for 24 h. The mixed calcined powders were then pressed into disks with a diameter of 15 mm at a pressure of 80 MPa. The pellets were sintered between 1050 and 1200 ^{o}C for 2 h and cooled in a furnace. X-ray diffraction (XRD; Philip PW3040/60 X' Pert Pro) was employed to identify the phase formed and the optimum temperature for the optimum formation of BNT-BKT-BT ceramics. The morphological features

of the product were imaged using scanning electron microscopy (SEM; LEO 1455 VP). The density of the sintered ceramics was measured by the Archimedes method. The average grain sizes were determined by using the mean linear intercept method. The raw data were obtained by measuring the grain sizes over 300 grains. Silver paste was coated and fired at 600 ^{o}C for 5 min to form electrodes and poled in a silicon oil bath at 80 ^{o}C for 15 min under a dc field of 35 kv/cm. The dielectric property before poling as a function of temperature was also observed using a LCR impedance analyzer (Agilent 4263B). The polarization hysteresis (P-E) loops were measured by using a ferroelectric test system (Radiant Technologies, Inc.). The piezoelectric constant (d_{33}) was measured using a quasistatic d_{33} meter (Berlincourt, Model CADT).

Results and discussion

The XRD diffraction patterns of sintered ceramics with various sintering temperatures are shown in Figure 1. The BNT-BKT-BT ceramics were identified as having a pure perovskite phase at all sintering temperatures. Generally, the rhombohedral symmetry is characterized by a (003)/(021) peak splitting between 38^{o} and 42^{o} and a single (202) peak between 45^{o} and 48^{o} (Chen *et al.*, 2008). While, the tetragonal symmetry, is identified by a single (111) peak between 38^{o} and 42^{o} and a (002)/(200) peak splitting between 45^{o} and 48^{o} (Chen *et al.*, 2008). In the case of this work, the tetragonal and rhombohedral symmetry of BNT-BKT-BT at the sintering temperature $\geq$ 1125 ^{o}C are characterized by the (002)/(200) and (003)/(021) peaks splitting in the 2θ range of 45-48^{o} and 39-41^{o}, respectively (Figure 2). So, it can be inferred that this composition lies in the MPB, where the rhombohedral and tetragonal phases coexist. This could be matched with JCPDS file number 36-0339 and 36-0340 and corresponded to previous work (Nagata *et al.*, 2003). The peak splitting of (003)/(021) between 38^{o} and 42^{o} and (002)/(200) between 45^{o} and 48^{o} did not distinctively appeare at the sintering temperature $\leq$ 1100 ^{o}C. This result may be because the BNT-BKT-BT ceramics were not fully crystallized at a low sintered temperature ($\leq$ 1100 ^{o}C).

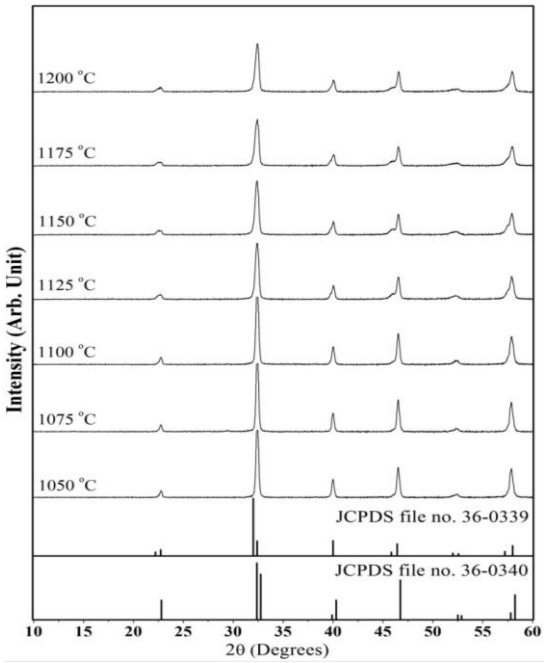

Figure 1 X-ray patterns of BNT-BKT-BT ceramic at various sintering temperatures in the 2θ range of 10^o to 60^o.

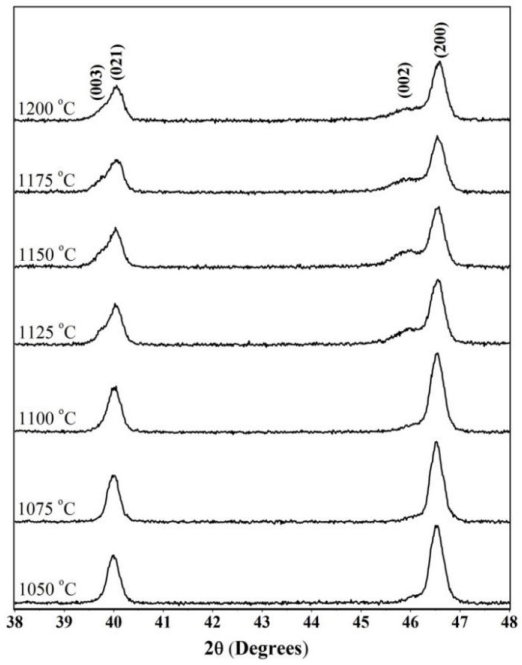

Figure 2 X-ray patterns of BNT-BKT-BT ceramic in the 2θ range of 38^o to 48^o.

Figure 3 illustrates the morphological changes in the BNT-BKT-BT surface of the sintered ceramics as a function of sintering temperatures. The point touches between particles grew into necks which exhibited the primary state of sintering at the sintering temperature ≤ 1100 ^{o}C, as shown in Figure 3 (a)-(b). The increasing of sintering temperatures up to 1100 ^{o}C caused no evident change in the microstructure except for a slight increase in the grain size. When the sintering temperature increased higher than 1100 ^{o}C and reached its highest at 1175 ^{o}C, the grain growth became increasingly active. At the same time, the pore structure decreased and led to an obvious change in the feature of grain size. The porosity of samples sintered at 1200 ^{o}C increased as shown in Figure 3 (f). The grain growth exhibited an almost similar rectangular morphology, as shown in Figure 3 (c)-(f). The average grain sizes increased from 1.03 to 3.49 μm when the sintering temperatures increased from 1050 to 1200 ^{o}C, as shown in Table 1.

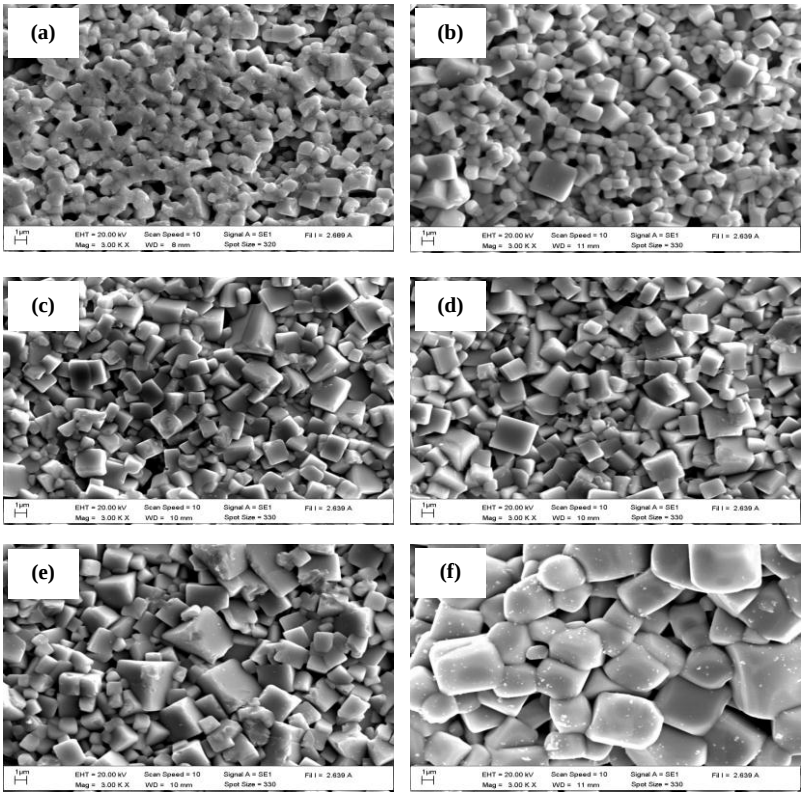

Figure 3 SEM photographs of BNT-BKT-BT ceramics sintered at; (a) 1075 ^{o}C, (b) 1100 ^{o}C, (c) 1125 ^{o}C, (d) 1150 ^{o}C, (e) 1175 ^{o}C and (f) 1200 ^{o}C.

The measured density with a variation of the sintering temperatures is shown in Table 1. The density first increased and reached its highest at 1175 ^{o}C and then dropped in value when the sintering temperature was higher than 1175 ^{o}C, as shown in Table 1. It was noticed that the density decreased when the firing temperature was higher than an optimal temperature in the sintering process. The maximum density was around 5.78 g/cm^3 or ~96.5% of the theoretical density obtained from the sintered sample at 1175 ^{o}C for 2 h. The percent of shrinkage of the pellet samples is listed in Table 1. The tendency of the percent of shrinkage had the same trend with the density as a function of sintering temperatures. The percent of shrinkage first increased and reached its highest at 1175 ^{o}C. Then, the percent of shrinkage of the ceramics decreased as the sintering temperatures increased above 1175 ^{o}C.

Table 1 The average grain size, density and shrinkage of BNT-BKT-BT samples.

Sintered temperature (^{o}C)	Average grain size (μm)	Density (g/cm^3)	Relative density (%)	Shrinkage (%)
1050	1.03±0.09	4.88	81.5	7.87
1075	1.06±0.12	5.14	85.8	10.13
1100	1.16±0.13	5.49	91.7	13.6
1125	1.36±0.26	5.64	94.2	15.93
1150	1.47±0.29	5.68	94.9	17.35
1175	1.71±0.53	5.78	96.5	17.48
1200	3.49±0.58	5.72	95.5	14.77

Figure 4 shows the temperature dependence of the dielectric constant (ε_r) and dielectric loss tangent of BNT-BKT-BT ceramics which were measured at 10 kHz. In the samples sintered at temperature ≤ 1100 ^{o}C, the dielectric constant showed a broadened peak around 262 ^{o}C, which was due to the phase transition from an antiferroelectric to paraelectric state (Takenaka *et al.*, 1991). In the samples sintered > 1100 ^{o}C, the dielectric constant showed 2 broadened peaks. The first broadened peak of various sintered samples showed an anomaly in a similar range of temperature as shown in Table 2, which was due to the phase transition from the ferroelectric to antiferroelectric state (Takenaka *et al.*, 1991). The second broadened peaks of each condition were above 265 ^{o}C, which was caused by an antiferroelectric-paraelectric transformation process. At Curie temperature, the maximum dielectric constant was observed in the samples, which first increased and reached its highest at 1175 ^{o}C and then dropped in value when the sintering temperature was higher than 1175 ^{o}C. The dielectric

loss at T_c is shown in Table 2. The samples sintered at temperature ≤ 1100 ^oC, showed only a peak may be caused because fully crystallization still has not formed. These results corresponded to the XRD results and density.

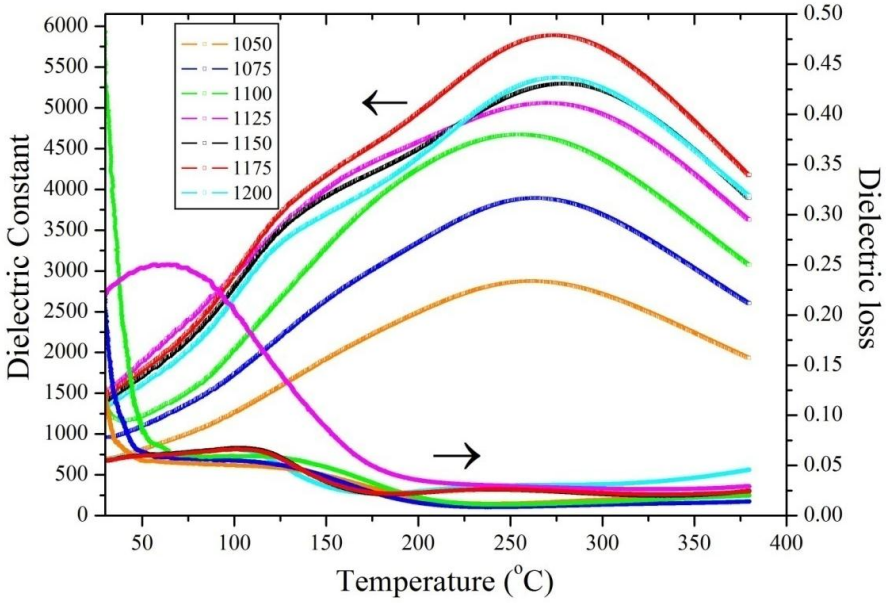

Figure 4 Temperature dependence of the dielectric constant and dielectric loss tangent of BNT-BKT-BT ceramics measured at 10 kHz.

The ceramics with the maximum density, which obtained when sintered at 1175^oC, were used to investigate ferroelectric and piezoelectric properties. Figure 5 shows the P-E hysteresis loop of a BNT-BKT-BT sample with different electric field strengths at room temperature. It is clearly seen that the shape of the hysteresis differ greatly with the electric field strength. A near-linear relationship of P–E is observed at 5 kV/cm electric field strength. This result is due to the fact that the electric field is not large enough to switch any domains. The polarization nonlinearity is improved in both regions of the positive and negative fields at 10 kV/cm electric fields. These demonstrated that the electric field strength of 10 kV/cm has enough energy to constrain realignment of some domains in the direction of the applied fields. The largest of symmetric hysteresis loop is revealed at 35 kV/cm electric field strength, which displays the remanent polarization (P_r) of 9.5 $\mu C/cm^2$ and coercive field E_c of 15.1 kV/cm. Due to the limiting of the based instrument, the saturated hysteresis loop has still not been obtained at 35 kV/cm electric field strength when compared with previous works (Takenaka *et al.*, 1991; Xu *et al.*, 2004; Wang *et al.*, 2005). For the piezoelectric constant, the sample (dwell at 1175 ^oC during 2 h) showed a

high piezoelectric constant around 156 pC/N. A high piezoelectric constant of 140 pC/N was shown by H. Nagata et al. (2003), who used the solid state reaction method for prepared BNBKT ceramics. The samples obtained from the combustion technique had a piezoelectric constant higher than the samples which were prepared via the solid state reaction method and used a lower sintering temperature (Nagata *et al.*, 2003). This demonstrated the efficiency of the combustion technique in the preparation of highly dense, dielectric and piezoelectric constant of BNT-BKT-BT ceramics.

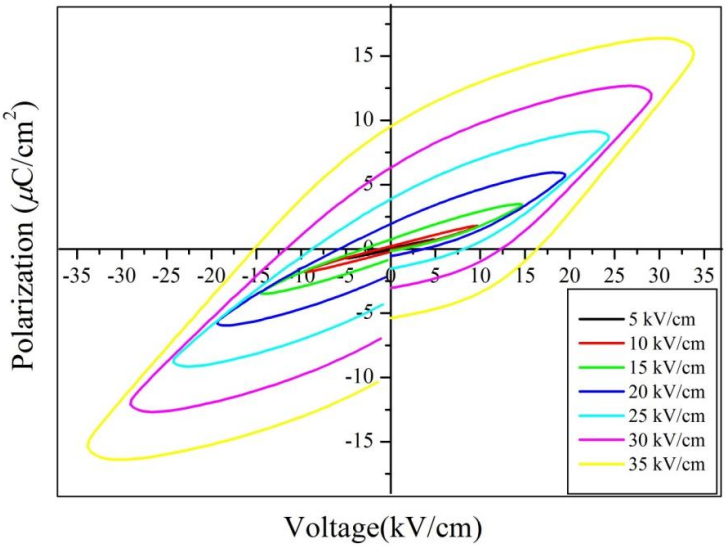

Figure 5 P-E hysteresis loop of BNT-BKT-BT ceramic sintered at 1175 ^{o}C.

Table 2 Range of depolarization temperature (T_d), curie temperature (T_c), dielectric constant (ε_r), and loss tangent (tan δ) of BNT-BKT-BT ceramics at various sintering temperature.

Sintered temperature (^{o}C)	Range of T_d (^{o}C)	T_c (^{o}C)	ε_r (at T_c)	tan δ (at T_c)
1050	-	261	2876	0.0126
1075	-	263	3894	0.0091
1100	-	254	4673	0.0110
1125	110-180	269	5059	0.0283
1150	105-176	280	5297	0.0234
1175	104-175	274	5890	0.0245
1200	100-170	276	5370	0.0305

Conclusions

High density, dielectric and piezoelectric properties in ceramics can be obtained successfully by the combustion method. The sintering temperatures directly affect phase composition, microstructure, density and the dielectric properties of the sintered ceramics. The range of the average grain size increased with the increase of sintering temperatures. The maximum densities ~96.5% of the theoretical density, dielectric constant at T_c and percent of shrinkage were obtained from the ceramics sintered at the optimal temperature of 1175 ^oC for 2 h. The high piezoelectric constant (156 pC/N), remanent polarization (9.5 $\mu C/cm^2$) and coercive field (15.1 kV/cm) were also obtained from the sample sintered at 1175 ^oC.

Acknowledgments

This work was supported financially by the Thailand Research Fund (TRF), Commission on Higher Education (CHE), Faculty of Science, Naresuan University. Thanks also to the Science Lab Center, Faculty of Science, Naresuan University for support facilities. Acknowledgements also to Mr. Don Hindle, for his helpful correction of the manuscript.

References

Chu, B.J., Chen, D.R., Li, G.R. and Yin, Q.R. (2002). Electrical properties of $(Na_{1/2}Bi_{1/2})TiO_3$–$BaTiO_3$ ceramics. *Journal of the European Ceramic Society*, *22*, 2115–2121.

Chen, M., Xu, Q., Kim, B.H., Ahn, B.K., Ko, J.H., Kang, W.J., et al. (2008). Structure and electrical properties of $(Na_{0.5}Bi_{0.5})_{1-x}Ba_xTiO_3$ piezoelectric ceramics. *Journal of the European Ceramic Society*, *28*, 843-849.

Elkechai, O., Manier,M. and Mercurio, J. P. (1996). $Bi_{0.5}Na_{0.5}TiO_3$–$Bi_{0.5}K_{0.5}TiO_3$ system: a structure and electrical study. *Physica Status Solidi (a)*, *157*, 499–506.

Ichinose, N. and Udagawa, K. (1995). Piezoelectric properties of $(Bi_{1/2}Na_{1/2})TiO_3$-based ceramics. *Ferroelectrics*, *169*, 317–325.

Julphunthong, P. and Bongkarn, T. (in press). Phase formation, microstructure and dielectric properties of $Ba(Zr_{0.1}Ti_{0.9})O_3$ ceramics prepared via the combustion technique. *Current Applied Physics*.

Nagata, H., Yoshida, M., Makiuchi, Y. and Takenaka, T. (2003). Large piezoelectric constant and high curie temperature of lead-free piezoelectric ceramic ternary system based on bismuth sodium titanate-bismuth potassium titanate-barium titanate near the morphotropic phase boundary. *Japanese Journal of Applied Physics*, *42*, 7401-7403.

Takenaka, T., Maruyama, K. and Sakata, K. (1991). $(Bi_{1/2}Na_{1/2})TiO_3$–$BaTiO_3$ system for lead-free piezoelectric ceramics. *Japanese Journal of Applied Physics*, *30*(9B), 2236–2239.

Takenaka, T., Okuda, T. and Takegahara, K. (1997). Lead-free piezoelectric ceramics based on $(Bi_{1/2}Na_{1/2})TiO_3$–$NaNbO_3$. *Ferroelectrics*, *196*, 175–178.

Takenaka, T. (1999). Piezoelectric properties of some lead-free ferroelectric ceramics. *Ferroelectrics*, *230*, 87–98.

Thongtha, A. and Bongkarn, T. (2009). Phase formation and microstructure of barium zirconate ceramics prepared using the combustion technique. *Ferroelectrics*, *383*, 33-39.

Thongtha, A. and Bongkarn, T. (2010). Fabrication and characterization of perovskite $SrZrO_3$ ceramics through a combustion technique. *Key Engineering Materials*, *421-422*, 223-226.

Wang, X.X., Or, S.W., Tang, X.G., Chan, H.L.W., Choy, P.K., and Liu, P.C.K. (2005). TiO_2-nonstoichiometry dependence on piezoelectric properties and depolarization temperature of $(Bi_{0.5}Na_{0.5})_{0.94}Ba_{0.06}TiO_3$ lead-free ceramics. *Solid State Communications*, *134*, 659-663.

Xu, Q., Chen, S., Chen, W., Wu, S., Lee, J., Zhou, J., et al. (2004). Structure, piezoelectric properties and ferroelectric properties of $(Na_{0.5}Bi_{0.5})_{1-x}Ba_xTiO_3$ system. *Journal of Alloys and Compounds*, *381*, 221-225.